Limits of Vinylidene Fluoride RAFT Polymerization

Marc Guerre, S. M. Wahidur Rahaman, Bruno Ameduri, Rinaldo Poli, Vincent Ladmiral

Limits of Vinylidene Fluoride RAFT Polymerization

Marc Guerre,[a] S. M. Wahidur Rahaman,[b] Bruno Améduri,[a] Rinaldo Poli,[b,c] Vincent Ladmiral[a]**

[a]Institut Charles Gerhardt, Ingénierie et Architectures Macromoléculaires, UMR 5253 CNRS, UM, ENSCM, Place Eugène Bataillon, UM, 34095 Montpellier Cedex 5 France.

[b]CNRS, LCC (Laboratoire de Chimie de Coordination), Université de Toulouse, UPS, INPT, 205 Route de Narbonne, BP 44099, F-31077 Toulouse Cedex 4, France.

[c]Institut Universitaire de France, 1, rue Descartes, 75231 Paris Cedex 05, France.

KEYWORDS: RAFT, Vinylidene Fluoride, Reversible deactivation radical polymerization, Xanthate, DFT calculations

ABSTRACT: The investigations reported in this article probe the behavior of the RAFT polymerization of vinylidene fluoride (VDF) when degrees of polymerization higher than 50 are targeted: they demonstrate that higher-molar-mass PVDF (11,000 g mol^{-1}) can indeed be prepared by RAFT polymerization, but only at rather low monomer conversions (< 33 %). This study more carefully examines the behavior of the reputedly non-reactive -CF_2CH_2-XA (where XA designates the xanthate group) formed by inverse VDF addition and known to accumulate in the reaction medium during the polymerization. A combination of ^{1}H and ^{19}F NMR spectroscopic monitoring and comprehensive DFT calculations of the various exchange and propagation reactions at work explains the unexpected behavior of this polymerization. The present study disproves entirely the

generally accepted belief that -CF_2CH_2-XA-terminated PVDF chains are "dead" and shows how these chains are reactivated, albeit slowly, throughout the polymerization. This activation occurs prevalently and counterintuitively through degenerative exchange by the minority PVDF-$CF_2CH_2^{\bullet}$ radicals. The resulting kinetic scheme rationalizes the experimentally observed absence, after conversion of all the dormant chains to the less reactive -CF_2CH_2-XA end-group, of the longer polymer chains expected from a free radical mechanism.

INTRODUCTION

Fluoropolymers (i.e. polymers the main chain of which is fluorinated), such as polytetrafluoroethylene (PTFE), poly(vinylidene fluoride) (PVDF) and poly(chlorotrifluoroethylene) (PCTFE) to name just a few, constitute a very important class of polymeric materials and have found numerous high added-value applications.[1,2] Fluoropolymers are usually prepared by radical polymerization. Ironically, while fluoroolefins were among the first monomers polymerized using reversible deactivation radical polymerization (RDRP) techniques,[3] the development of well-defined architectures based on fluoropolymers is clearly lagging behind that of more widespread vinyl monomers (styrene, acrylics…). This is probably due to the fact that most fluoroolefins are gases under Standard Temperature and Pressure, thus requiring less common equipment such as pressure reactors, and to their specific reactivity due to the fluorine atoms, which exert both strong σ-inductive electron-withdrawing and π-donating effects.[4]

PVDF is the second most produced fluoropolymer after PTFE. PVDF and VDF copolymers have found numerous applications, for example in filtration membranes,[5] architectural coatings, fuel hoses, liners, wire and insulation, and their electroactive properties have the potential to mr

open new high-technology markets.[6-8] Recent years have witnessed a growing interest for the development of efficient preparation methods of well-defined fluoropolymer-based architectures.[9]

Iodine Transfer Polymerization (ITP)[10] and RAFT/MADIX[11] polymerization have emerged as the most efficient techniques to control the polymerization of fluoroolefins[12-20] and to prepare well-defined fluoropolymer architectures. We recently reported the results of our detailed investigations of the RAFT polymerization of VDF.[19] That study clearly showed that xanthates chain transfer agents (CTA) are very efficient for preparing PVDF with narrow molar mass distributions (Đ < 1.5). These well-defined xanthate-terminated PVDF can easily be converted into macromonomers, opening the way to novel fluorinated architectures.[21] However, the radical polymerization of VDF is accompanied by a non-negligible amount of chain inversions, head-to-head (HH) VDF additions. These reverse additions are detrimental to the preparation of well-controlled PVDF chains using ITP or RAFT. It has indeed been proven that chain-ends terminated by an inversely added VDF unit accumulate in the reaction medium relatively rapidly.[14,19,22] These PVDF chains are also believed not to be able to participate into further degenerative transfer. Asandei et al.[14] reported a method, based on the use of $Mn_2(CO)_{10}$, to reactivate unreactive iodine-capped chain-ends and to successfully extend PVDF chains under free radical polymerization conditions. In addition, polymerization of VDF in hydrogenated solvents is also affected by undesirable transfer-to-solvent reactions. This H-abstraction results in losses of CTA and chain-end functionality, and in some cases in the generation of undesired additional polymer chains.[19] Our previous report[19] gave thorough evidence for all these phenomena, but restricted the investigation to short polymer chains (target $DP_n < 50$). The present research explores the limits of the RAFT polymerization of VDF and describes how higher-molar-mass PVDF can be prepared. In the course of these investigations, we were prompted to examine the fate of the PVDF chains that are terminated with an inversely added VDF unit. Our study, combining experimental observations and DFT

calculations, proves that these reputedly inactive chains are not “dead”, and shows how they are reactivated throughout the polymerization.

EXPERIMENTAL SECTION

Materials

All reagents were used as received unless stated otherwise. 1,1-Difluoroethylene (vinylidene fluoride, VDF) was kindly supplied by Arkema (Pierre-Benite, France). *O*-ethyl-*S*-*(*1-methoxycarbonyl)ethyldithiocarbonate (CTA_{XA}) was synthesized according to the method described by Liu et al.[23] *Tert*-amyl peroxy-2-ethylhexanoate (Trigonox 121, purity 95%) was purchased from AkzoNobel (Chalons-sur-Marne, France). ReagentPlus grade (purity > 99%) dimethyl carbonate (DMC), and laboratory reagent grade hexane (purity > 95%) were purchased from Sigma Aldrich and used as received.

Characterization

Nuclear Magnetic Resonance

Nuclear Magnetic Resonance (NMR) spectra were recorded on a Bruker AC 400 instrument. Deuterated acetone was used as the solvent for all samples. Coupling constants and chemical shifts are given in hertz (Hz) and part per million (ppm), respectively. The experimental conditions for recording ^{1}H and ^{19}F NMR spectra were as follows: flip angle 90° (or 30°), acquisition time 4.5 s (or 0.7 s), pulse delay 2 s (or 2 s), number of scans 128 (or 512), and a pulse width of 5 μs for ^{19}F NMR.

Size Exclusion Chromatography

Size exclusion chromatograms (SEC) were recorded using a triple detection GPC from Agilent Technologies with its corresponding Agilent software, dedicated to multi-detector GPC

calculation. The system used two PL1113-6300 ResiPore 300 x 7.5 mm columns with DMF (containing 0.1 wt % of LiCl) as the eluent with a flow rate of 0.8 $mL.min^{-1}$ and toluene as flow rate marker. The detector suite comprised a PL0390-0605390 LC light scattering detector with 2 diffusion angles (15° and 90°), a PL0390-06034 capillary viscometer, and a 390-LC PL0390-0601 refractive index detector. The entire SEC-HPLC system was thermostated at 35°C. PMMA standards were used for the calibration. The typical sample concentration was 10 mg/mL.

Autoclave

The polymerizations of VDF were performed in a 100 mL Hastelloy Parr autoclave systems (HC 276), equipped with a mechanical Hastelloy stirring system, a rupture disk (3000 PSI), inlet and outlet valves, and a Parr electronic controller to regulate the stirring speed and the heating. Prior to reaction, the autoclave was pressurized with 30 bars of nitrogen to check for leaks. The autoclave was then put under vacuum ($20 \cdot 10^{-3}$ bar) for 30 minutes to remove any trace of oxygen. A degassed solution of solvent, initiator and CTA_{XA} was introduced via a funnel under vacuum. The reactor was then cooled down using a liquid nitrogen bath and VDF was transferred by double weighing (*i.e.* mass difference before and after filling the autoclave with VDF). After warming up to ambient temperature, the autoclave was heated to the target temperature under mechanical stirring.

Synthesis

RAFT Homopolymerization of Vinylidene Fluoride (VDF) (Scheme 1)

Using the experimental setup described above, a typical polymerization (run 5 in Table 1) of VDF was performed as follows: A solution of Trigonox 121 (158 mg, 6.87 10^{-4} mol) and CTA_{XA} (1.30 g, 6.25 10^{-3} mol) in DMC (60 mL), was degassed by N_2 bubbling during 30 min. This homogenous solution was introduced into the autoclave using a funnel, VDF gas (19.0 g, 0.297 mol) was transferred in the autoclave at low temperature, and the reactor was gradually heated to

73 °C. The reaction was stopped after 20 h. During the reaction, the pressure increased to a maximum of 25 bars and then decreased to 10 bars after 20 h.

Scheme 1. Schematic representation of the RAFT Polymerization of VDF.

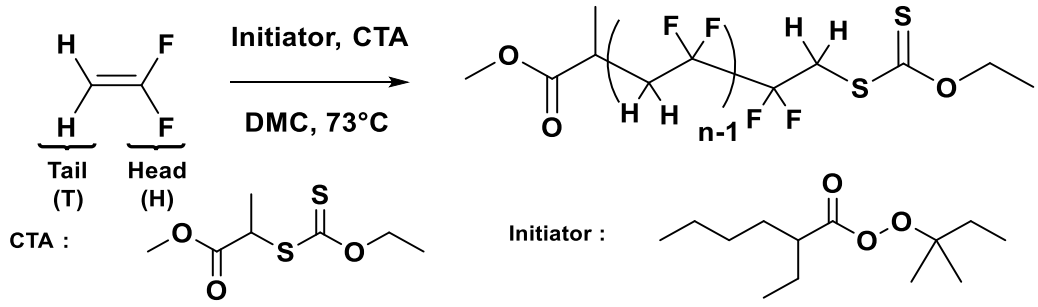

The autoclave was cooled down to room temperature (ca. 20 °C), purged from the residual monomers, and the dimethylcarbonate solvent was removed under vacuum. The crude product was dissolved in 30 mL of warm THF (ca. 40 °C), and left under vigorous stirring for 30 minutes. This polymer solution was then precipitated from 400 mL of chilled hexane. The precipitated polymer (white powder) was filtered through a filter funnel and dried under vacuum ($15 \cdot 10^{-3}$ bar) for two hours at 50 °C. The polymerization yield (65 %) was determined gravimetrically (mass of dried precipitated polymers / mass of monomer introduced in the pressure reactor). Yields were used as conversion, since conversion is very difficult to measure accurately for VDF or other gaseous monomers.

^{1}H NMR (400 MHz $(CD_3)_2CO$, δ (ppm)) : 1.19-1.24 (d, -CH(C**H$_3$**)(C=O)-, $^3J_{HH}$= 7.1 Hz), 1.40-1.46 (t, -S(C=S)O-CH_2-C**H$_3$**, 1.65-1.85 (m, -CF_2-C**H$_3$**), $^3J_{HH}$= 7.2 Hz), 2.28-2.43 (m,-CF_2-C**H$_2$**-C**H$_2$**-CF_2-, VDF-VDF TT (tail-to-tail) reverse addition), 2.70-3.19 (t, -CF_2-C**H$_2$**-CF_2-, VDF-VDF HT (head-to-tail) regular addition), 3.60-3.69 (s, -(C=O)-O-C**H$_3$**), 4.02-4.17 (t, -CF_2-C**H$_2$**-S(C=S)OEt, $^3J_{HF}$= 18 Hz), 4.67-4.77 (q, (-S(C=S)O-C**H$_2$**-CH_3, $^3J_{HH}$= 7.2 Hz), 6.05-6.45 (tt, $^2J_{HF}$= 55 Hz , $^3J_{HH}$= 4.6 Hz -CH_2-CF_2-**H**).

^{19}F NMR (376 MHz $(CD_3)_2CO$, δ (ppm)) : -115.63 (-CH_2-CF_2-C**F₂**-CH_2-CH_2-, VDF-VDF HH reverse addition), -114.29 ($^2J_{HF}$= 55 Hz, -CH_2-C**F₂**-H), -113.34 (-CH_2-C**F₂**-CF_2-CH_2-CH_2-, HH reverse addition), -113.09 (CH_2-CF_2-**C**F₂-CH_2-S-), -112.69 (-CH_2-**C**F₂-CF_2-CH_2-S-), -94.79 (-CH_2-CH_2-C**F₂**-CH_2-, TT reverse addition), -107.7 (-CF_2-C**H₃**), -93.50 (-CH_2-C**F₂**-CH_2-$CH(CH_3)$(C=O)-), -92.12 (-CH_2-C**F₂**-CH_2-CF_2H), -91.44 (-CH_2-CH_2-CF_2-CH_2-**C**F₂-CH_2-CF_2-, regular VDF-VDFHT addition), -91.00 (-CH_2-C**F₂**-CH_2-, regular VDF-VDF HT addition).

Computational details

The computational work was carried out using the Gaussian09 suite of programs.[24] The geometry optimizations were performed in the gas phase without any symmetry constraint using the B3PW91 functional in combination with the 6-31G(d,p) basis functions for all atoms. The unrestricted formulation was used for all radicals, yielding negligible spin contamination in all cases. The ZPVE, PV and TS corrections at 298 K were obtained with Gaussian09 from the solution of the nuclear equation using the standard ideal gas and harmonic approximations at T = 298.15 K, which also verified the nature of all optimized geometries as local minima or first order saddle points. A correction of 1.95 kcal/mol was applied to all G values to change the standard state from the gas phase (1 atm) to solution (1 M).[25]

Determination of the VDF concentration in DMC at 73 °C under 33.1 bar

The autoclave was put under vacuum ($20 \cdot 10^{-3}$ bar) for 30 minutes to remove any trace of oxygen. Dimethylcarbonate (37 g, 34.6 mL) was introduced via a funnel under vacuum. The reactor was then cooled down using a liquid nitrogen bath and VDF (21.0 g) was transferred by double weighing. The autoclave was heated up to 73 °C under stirring. After 30 min, a constant pressure of 33.1 bar was recorded. Then the autoclave was cooled down to room temperature (ca. 20 °C), purged from monomers and solvent. Exactly the same volume of lead balls (34.6 mL) was placed

in the reactor and the total weight was recorded. 17 g of VDF were then introduced in the reactor following the protocol described above, and the autoclave was heated up to 73 °C until reaching constant pressure. VDF was then progressively removed from the reactor until the pressure reached 33.1 bars. The reactor was then weighed again. The mass of VDF contained in the free volume of the reactor at P = 33.1 bars and T = 73 °C was calculated to be 9.5 g. The solubility of VDF in DMC at P = 33.1 bars and T = 73 °C was obtained as (21 – 9.5) / (64.02 x 34.6 10^{-3}) = 5.2 mol L^{-1}.

RESULTS AND DISCUSSION

Assessment of the apparent chain transfer constant of VDF towards CTA_{XA}

Although RAFT polymerization was shown to efficiently control the polymerization of VDF,[19] there is a clear lack of kinetic data related to this polymerization. We thus assessed the apparent transfer constant of VDF towards *O*-ethyl-*S*-(1-methoxycarbonyl)ethyldithiocarbonate (CTA_{XA}, Scheme 1) using O'Brien and Gornick's method (Figure S1).[26] This method gave a $C_{Tr(app)}$ value of 49 at 73 °C confirming the efficient transfer of PVDF radicals to the RAFT chain transfer agent used. It is important to note that the transfer constant determination method used here does not take into account the reversibility of the addition onto CTA_{XA}, the real transfer constant is therefore likely higher than 49.[27] The same method used for the ITP of VDF (at 75°C) reported $C_{Tr(app)}$ values for $HCF_2CF_2CH_2I$ and $C_6F_{13}CH_2CF_2I$ of 0.3 and 7.4 respectively.[28] These results confirm that CTA_{XA} is a much better CTA than alkyl iodides.

Investigations of the ability of the RAFT process to produce high molar mass PVDF

To test the capacity of the RAFT polymerization of VDF to afford high molar mass PVDF, three polymerizations targeting different DP_n (50, 100 and 200) were examined. As reported

previously,[19] HH additions were shown to lead to an accumulation of -CF_2-CH_2-XA-terminated PVDF chains, henceforth noted as $PVDF_T$-XA (where -XA designates the *O*-ethyl xanthate group: -SC(S)OCH_2CH_3). Conversely, -CH_2CF_2-XA-terminated chains will be noted $PVDF_H$-XA. The evolution of the PVDF chain-ends was thus carefully monitored by ^{1}H.[29] for each polymerization (see Table 1, and Figure S2 for the assignment of the ^{1}H NMR signals), and compared to the corresponding first-order kinetic plots (Figure 1). These kinetic plots (Ln($[VDF]_0$ / [VDF]) *vs* t), (Figure 1, bottom) showed four polymerization regimes: (i) an induction period where the polymerization rate is almost negligible,[30] maybe caused by slow initiation of VDF by the R$^\bullet$ radical, followed by (ii) polymerization at a relatively slow rate (which increases upon decreasing $[VDF]_0/[CTA]_0$ ratios as is often observed during RAFT polymerizations),[31] (iii) a significant increase in the rate of polymerization, and (iv) a plateau where the polymerization progresses very slowly or even stops. This plateau, which had not been described in earlier reports, occurs at similar VDF conversions (ca. 65 %) and may be caused by the pressure drop inside the reactor below the vapor pressure (and critical pressure) of VDF, which decreases the VDF concentration in solution. The other 3 phases observed in the RAFT polymerizations of VDF have been described before.[19]

Table 1. Experimental Conditions and Results for the RAFT polymerization of VDF in the presence of CTA_{XA}.

Run	$[VDF]_0/[CTA]_0$	Reaction Time	[a]yield %	[b]$DP_{(NMR)(R)}$	[c]$M_{n(theo)}$ (g/mol)	[d]$M_{n(NMR)(R)}$ (g/mol)	[e]$M_{n(SEC)}$ (g/mol)	[e]Đ	[b]-CF_2-CH_2-XA %	[b]-CH_2-CF_2-XA %	[b]CF_2H %	[b]-CF_2-CH_3 %	[b]DMC-CH_2-CF_2- %	[b]R-CH_2-CF_2- %
1	50	5h	< 5	4	n.d.	500	800	1.05	20	74	6	0	0	100
2	51	10h	25	20	1000	1500	3900	1.12	38	47	15	0	0	100
3	51	15h	35	29	1400	2100	4100	1.29	60	29	11	< 1	0	100
4	47	17.5h	[f]**45**	41	1600	2800	5300	1.30	**86**	**2**	**12**	**< 1**	0	100

5	54	20h	65	47	2400	3200	7200	1.40	85	0	n.d	n.d	0	100
6	48	24h	65	44	2200	3000	5000	1.42	86	0	n.d	n.d	0	100
7	100	2.5h	10	7	900	700	1100	1.10	32	64	4	0	0	100
8	100	5h	22	36	1700	2600	3800	1.33	54	26	16	4	0	100
9	100	7.5h	f_{32}	69	2300	4700	6900	1.43	**71**	**0**	**25**	**4**	4	96
10	100	10h	52	92	3600	6100	8700	1.44	61	0	n.d	n.d	7	93
11	100	20h	66	104	4500	6900	10100	1.50	50	0	n.d	n.d	12	88
12	200	5h	8	33	1300	2400	6500	1.24	30	57	10	3	0	100
13	200	7h	26	56	3600	3800	10100	1.33	63	13	21	3	<1	100
14	200	8h	f_{33}	168	4500	11000	17000	1.37	**59**	**0**	**17**	**24**	7	93
15	200	10h	52	212	6900	13800	18000	1.41	49	0	n.d	n.d	17	83
16	n.a	16h	75	n.a	n.a	n.a	12400	2.10	n.a	n.a	n.a	n.a	n.a	n.a

Reactions conditions: Chain Transfer Agent (CTA) = CTA_{XA}, Initiator (I) = Trigonox 121, [I]/[CTA] = 0.1 (runs 1-15) [I]/[VDF] = 0.005 (run 16), T = 73 °C, Solvent = DMC. [a]Determined gravimetrically. [b]Determined by ^{1}H NMR using equations S1 to S6. [c]Calculated using yield as conversion. [d]Calculated from $DP_{(NMR)}$. [e]Determined by SEC. [f]Point where all $PVDF_H$-XA have disappeared. n.d stands for not determined. n.a. stands for not applicable.

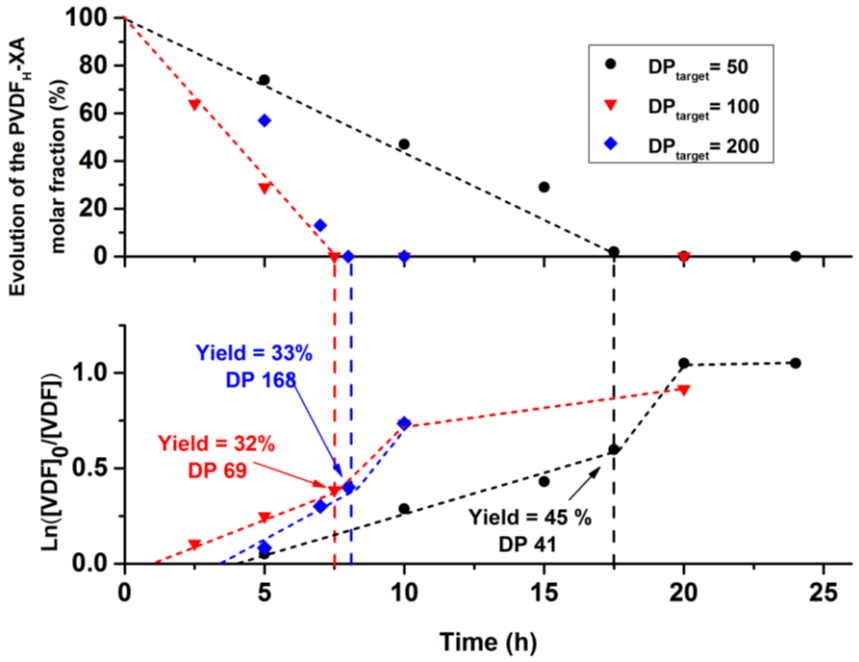

Figure 1. Correlation between the evolution *vs* time of the proportion of $PVDF_H$-XA chains (-CH_2-CF_2-XA-terminated PVDF chains) (top), and the corresponding first order kinetic plot (bottom) for three VDF RAFT polymerizations: DP_{target} = 50 (black), DP_{target} = 100 (red) and DP_{target} = 200 (blue).

However, the sharp increase in the rate of polymerization had been tentatively explained by an increase in the local VDF concentration caused by a change in the solubility of PVDF upon increase of its molar mass. The correlation between the evolution of $PVDF_H$-XA chains and the polymerization kinetics presented here (Figure 1) proves this interpretation to be incorrect, even though PVDF is indeed insoluble in DMC, even at 73 °C. Figure 1 clearly shows that the sharp increase in the rate of polymerization starts exactly when all the PVDF chains have been converted into $PVDF_T$-XA chains (at t =17.5 h for DP_{target} = 50, t = 7.5 h for DP_{target} = 100 and t = 8 h for DP_{target} = 200). This observation thus rather suggests that the polymerization rate increase is related to a change in the polymerization mechanism. These PVDF chains terminated by an inversely added VDF unit are believed[14,19,22] to be quasi unreactive vis-à-vis the degenerative chain transfer process at the heart of RAFT or ITP. It follows that the degenerative chain transfer (DT) should stop (or become negligible) when the last $PVDF_H$-XA chain has disappeared. If this were true, at this stage the remaining radicals and the newly formed radicals (from the thermal initiator) should have no choice but to polymerize the remaining VDF via free radical polymerization, thus forming PVDF chains that do not bear either R- or Z-group from the CTA.

This change in the polymerization mechanism from DT to free radical polymerization should also be observed in the plots of the evolutions of molar mass and dispersity versus conversion (Figure 2), and in the evolution of the GPC traces versus conversion (Figure 3). Figure 2 does show a slope change in the molar mass evolution versus conversion after the disappearance of the

last $PVDF_H$-XA (at conversion = 45 % for DP_{target} = 50; 32 % for DP_{target} = 100; and 33 % for DP_{target} = 200). However, this slope change is towards a slower increase of molar masses with conversion and it is not accompanied by a significant dispersity increase. If free radical polymerization was indeed taking place instead of RAFT polymerization, higher molar masses and dispersities would be expected (Run 16, Table 1).

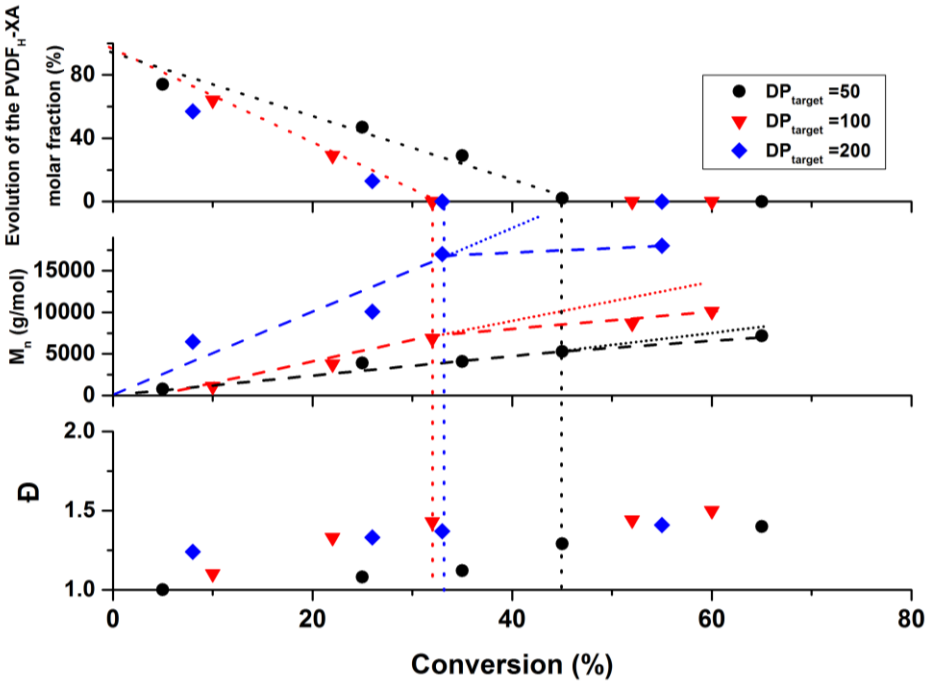

Figure 2. Correlation between the evolution of the proportion of $PVDF_H$-XA chains (top), of the molar mass (middle) and of the dispersity *vs* conversion for three VDF RAFT polymerizations: DP_{target} = 50 (black squares), 100 (red triangles) and 200 (blue triangles). Molar masses and dispersity were determined by GPC. Vertical dotted and dashed lines underline the mechanistic transition occurring when all the $PVDF_H$-XA chains have been converted into $PVDF_T$-XA chains.

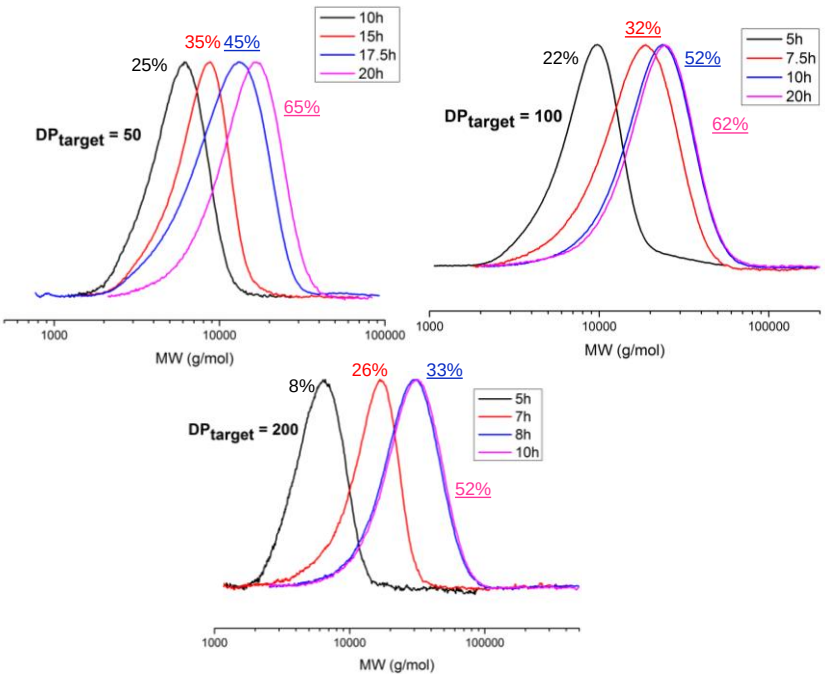

Figure 3. DMF GPC chromatograms of PVDF prepared by RAFT and targeting three degrees of polymerization: DP_{target} = 50 (top left), DP_{target} = 100 (top right) and DP_{target} = 200 (bottom). Corresponding conversions are shown next to each trace. The underlined conversions correspond to points where the polymerization medium no longer contains $PVDF_H$-XA.

The evolution of the GPC chromatograms versus conversion (Figure 3) is also affected by the disappearance of the $PVDF_H$-XA chains. After the transition point (where all xanthate-terminated PVDF chains are $PVDF_T$-XA), the maximum of the chromatograms (M_p) no longer increases as it would under an RDRP mechanism. This is consistent with the end of the DT-controlled chain growth. However, continuation of monomer conversion by free radical polymerization should generate high molar mass new polymer chains, which should appear as secondary molar mass distributions in the chromatograms. Indeed, after the transition points, the polymerizations converted about 20 % of VDF. If this polymerizations proceeded by a free radical mechanism, this would imply that the GPC traces of the final PVDF (Figure 3) correspond to mixtures of PVDF

produced by RAFT polymerization and of PVDF produced by free radical polymerization in the following wt % proportions : 69/31 (for DP_{target} = 50), 48/52 (for DP_{target} = 100) and 63/37 (for DP_{target} = 200). Moreover, the VDF/Initiator molar ratios at the transition points were calculated to be 840 (DP_{target} = 50), 1030 (DP_{target} = 100) and 2100 (DP_{target} = 200). Such significant ratios and conversions would undoubtedly yield PVDF of high molar mass and broad dispersity.

Such additional high molar mass distributions are not observed, not even as shoulders of the main distribution. These observations (or lack thereof) suggest that, beyond the transition point, the VDF polymerization proceeds neither under control by an RDRP mechanism nor as a pure free radical polymerization. To elucidate this surprising behavior, the propagation, chain inversion and reactivation rates were investigated using DFT calculations (vide infra).

Regardless of this mechanistic transition and its origin, the present study shows that higher molar mass, well-defined PVDF can be prepared using RAFT polymerization. Well-defined PVDF with DP = 41, 69 and 168 were synthesized when DP = 50, 100 and 200 were targeted respectively (Figure 1 and Table 1). However, the study clearly shows that well-controlled PVDF (i.e. with optimum chain-end functionality and containing only negligible quantities of polymer chains formed after the transition point) can only be prepared at relatively low VDF conversion and that the preparation of well-defined high molar mass PVDF can only be done at the detriment of conversion. Indeed, the disappearance of the last $PVDF_H$-XA chain occurs at a conversion around 45 % for DP_{target} = 50 and ca. 33 % for DP_{target} = 100 or 200.

Study of the chain defects evolution during the RAFT polymerization of VDF

The evolution of the chain defects (head-to-head and tail-to-tail additions) proportion as a function of conversion was also monitored. Since the proportion of defects in PVDF only depends

on the reaction temperature,[32] longer chains should display a higher number of intra-chain defects than shorter chains prepared at the same temperature. Indeed, the average number of monomer additions occurring per chain between two degenerative transfers increases with increasing $[VDF]_0/[CTA]_0$ initial ratios. Figure 4 shows the plots of the proportion of intrachain and total HH additions versus conversion. As expected, the amount of intrachain VDF HH additions increases with conversion and with increasing targeted degree of polymerizations (DP_{target}).

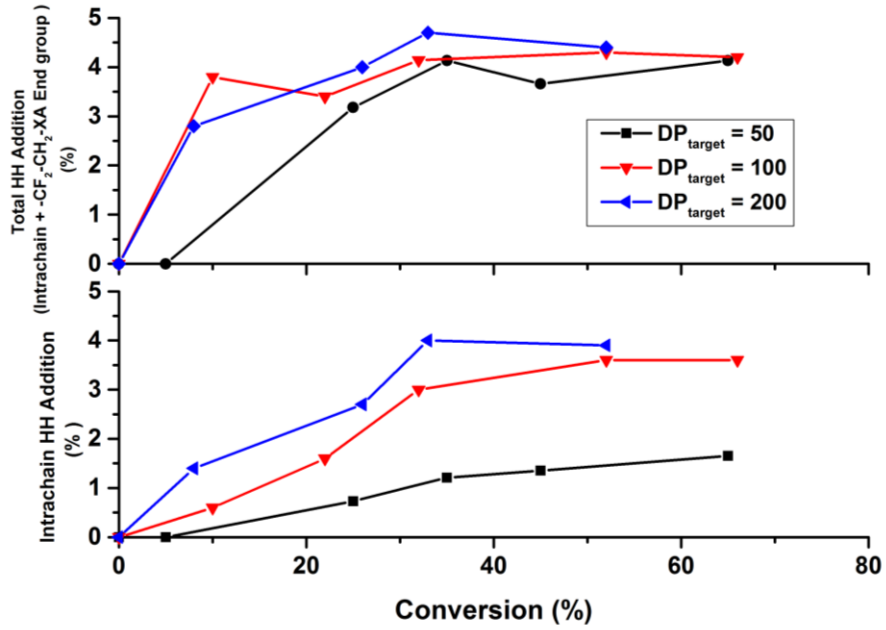

Figure 4. Evolution of the proportion of intrachain (bottom) and total (top) HH VDF additions *vs* conversion for three RAFT polymerizations of VDF: DP_{target} = 50 (black squares), DP_{target} = 100 (red triangles) and DP_{target} = 200 (blue triangles).

The total amount of HH VDF additions (intrachain + chain-end) stabilizes to identical proportion (ca. 4.1 %) for the three polymerizations examined. This value is in good agreement with the previously reported proportion of defects for polymerizations carried out at similar temperatures.[32-33]

Evolution of the PVDF chains functionality made by RAFT

Finally, we monitored by NMR the evolution of all chain-end groups for the PVDF made by RAFT polymerization with DP_{target} = 100. The results of this investigation are summarized in Figure 5. As observed and reported before,[19] $PVDF_H$-XA are progressively converted into $PVDF_T$-XA, and the overall end-group functionality decreases due to a slowly increasing amount of transfer to DMC (H-abstraction). Whereas new polymer chains initiated by the resulting DMC radicals were not observed in our previous study, here on the contrary DMC-initiated PVDF chains were detected, but only significantly after all the PVDF chains were converted into $PVDF_T$-XA (Figure S3). These chains give ^{1}H NMR signals characteristic of the CH_3 (singlet at 3.73 ppm) and of the CH_2 (triplet at 4.34 ppm) of the CH_3-O(C=O)-O-CH_2-PVDF α-end-group (Figure S2). Remarkably, the DMC radicals seemed to add exclusively to the CH_2 of VDF.

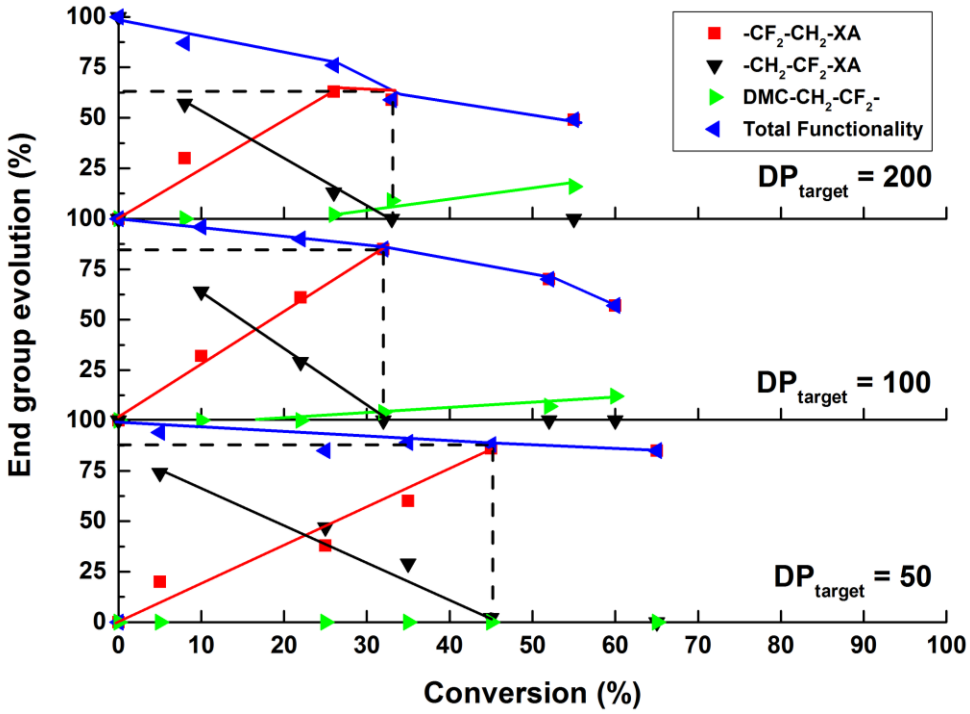

Figure 5. Evolution of the PVDF chains end-group functionality (-CH_2-CF_2-XA, -CF_2-CH_2-XA) and of the proportion of DMC-initiated PVDF chains *vs* time for RAFT polymerizations of VDF targeting different DP: DP_{target} = 50 (bottom), DP_{target} = 100 (middle), DP_{target} = 200 (top).

The formation of these DMC-initiated PVDF chains is accompanied by a gradual disappearance of the chain-ends (loss of xanthate group) of the $PVDF_T$-XA chains. These phenomena start with the mechanistic transition mentioned above (Figure 1 and Figure 5). The formation of increasing amounts of -CF_2-CH_3 end-groups after this transition (Figure S2 and S4) was also detected. These observations suggest that after the mechanism transition, transfer to DMC becomes more prevalent and that the thus formed DMC radicals not only initiate new PVDF chains, but also readily remove the xanthate groups from the $PVDF_T$-XA chains. This transfer reaction, however, seems to be irreversible and to lead to small DMC-xanthate adducts that are removed from the final polymer upon purification by precipitation, as shown previously.[19]

Computational study

a. General considerations, choice of models and computation level.

The above described, unexpected experimental findings raised several mechanistic questions, the most important one being to understand what happens when all PVDF chains are converted into $PVDF_T$-XA. To shed light on this phenomenon, DFT calculations were carried out on model systems. Previous studies have amply demonstrated the value of DFT for rationalizing unexpected phenomena in RDRP, particularly in RAFT,[34] ATRP,[35] OMRP,[36] and NMP.[37] Calculations on the polymerization of VDF by the RAFT method have not been previously reported, to the best of our knowledge.

To keep the calculations manageable in terms of computational effort while obtaining results of indicative value, the polymer chains were simplified to an H atom beyond the terminal monomer unit. Thus, the PVDF-$CH_2CF_2^{\bullet}$ (or $PVDF_H^{\bullet}$) and PVDF-$CF_2CH_2^{\bullet}$ (or $PVDF_T^{\bullet}$) chains were modeled by $CH_3CF_2^{\bullet}$ and $CHF_2CH_2^{\bullet}$, respectively. In the xanthate group, for the same reason of computational economy, the ethyl substituent was simplified to a methyl group, -$SC(S)OCH_3$. These structural modifications are not expected to introduce any major electronic change (polarity, homolytic strength) or steric effect in the bonds that are involved in the computed processes.

It must be emphasized that the main objective of the computational approach is not that of quantitatively reproducing observed data, but rather to provide insight into the occurring chemical processes. The values of DFT-calculated energy changes associated to chemical processes rarely deviate by less than a couple of kcal/mol from the experimentally available ones. DFT calculations provide better information when comparing data for closely related systems, because energy trends are reproduced more faithfully than absolute values. For this reason, we have not made a major effort in testing a variety of different functionals and basis sets in order to choose the most suitable method for the systems of interest. The theory level selected for our study (B3PW91/6-31G(d,p)) is commonly used for high-level calculations on organic and organometallic systems. However, we have initially benchmarked this method against available experimental data. All the results obtained from the computational study (energy, enthalpy and Gibbs energy at 298.15 K, Gibbs energy extrapolated to 343.5 K, Cartesian coordinates and views of the optimized geometries) are collected in tabular form in the SI.

b. Benchmarking on VDF free radical propagation.

The values of $k_p/k_t^{1/2}$ (0.14 $L^{1/2}$ $mol^{-1/2}$ $s^{-1/2}$ in 1,1,1,3,3-pentafluorobutane at 74 °C)[8,28] and k_p (19,400 L mol^{-1} s^{-1} at 60 °C and 1000 bar in supercritical CO_2)[38] for the VDF polymerization have

been reported, but individual k_p and k_t values in solution are not available to the best of our knowledge. Notably, it would have been interesting to compare the calculated propagation Gibbs energy barrier ($\Delta G_p^{\ddagger}$) with that derived from k_p using the Eyring equation. However, it is experimentally known that the most probable chain carrier is $PVDF_H^{\bullet}$ and that the most probable monomer addition mode is HT, conserving the nature of this reactive chain end, while the HH diads are present only at a level of 3.5-6 %[31,39]. We have calculated the profiles for all four possible types of radical addition to monomer, as shown in Figure 6. Figure 6a illustrates the energy profiles for the $PVDF_H^{\bullet}$ model radical additions to VDF in both HT and HH modes, while Figure 6b shows the profiles for the TH and TT additions of the $PVDF_T^{\bullet}$ model radical.

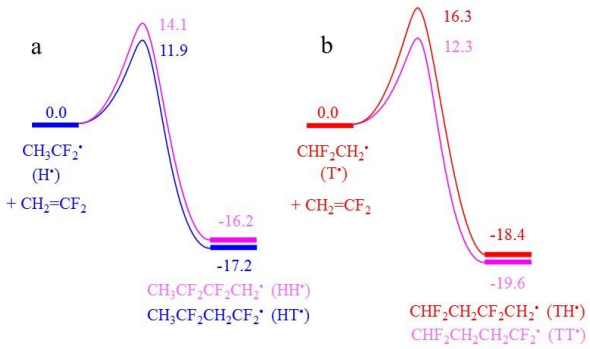

Figure 6. Energy profiles for (a) the HT and HH additions of the $PVDF_H^{\bullet}$ model radical, and (b) the TH and TT additions of the $PVDF_T^{\bullet}$ model radical to VDF. The reported values are $\Delta G°_{298.15}$ (1 M standard state) in kcal/mol.

Of all four possible addition modes, the lowest barrier is indeed, as known from the experimental evidence, that of the HT addition (11.9 kcal/mol), while the barrier of the alternative HH addition is ca. 2.2 kcal/mol higher (14.1 kcal/mol). This $\Delta(\Delta G)$ allows the prediction of a 2.4 % HH error probability at 298.15 K or 3.2 % after extrapolation of $\Delta(\Delta G)$ to the polymerization temperature (73 °C). These values are quite consistent with the experiment. The energy difference between the

two isomeric HT and HH transition states is carried over to the isomeric products. This difference results from the different C-C bond strengths of the CF_2-CH_2 and the CF_2-CF_2 bonds formed by HT and HH coupling, respectively, and/or from the different stabilization of the resulting $CH_2^{\bullet}$ and $CF_2^{\bullet}$ radicals. Concerning the $PVDF_T^{\bullet}$ model radical addition, the TT mode is more favored (12.3 kcal/mol) than the TH mode (16.3 kcal/mol). This is again in line with the experimental evidence, since the HT/HH/TT triad is, by far, much more frequent than the HT/HH/TH triad. This latter triad has indeed never been detected by NMR spectroscopy. Hence, generation of an inverted radical chain end is more likely followed by a TT addition (98.8 % probability according to the calculated barriers) to regenerate the preferred $PVDF_H^{\bullet}$ chain end. Similar results were also previously obtained, in reference to an uncontrolled VDF telomerization process, at a slightly different computational level (using the B3LYP functional) and with use of CF_3 instead of H as chain end.[40] The E barriers reported here with the use of BP86 are slightly and systematically smaller (by 0.5-1.5 kcal/mol) than those obtained with B3LYP, but their relative order is the same for both investigations: $\Delta E^{\ddagger}_{p,TT} < \Delta E^{\ddagger}_{p,HT} < \Delta E^{\ddagger}_{p,HH} < \Delta E^{\ddagger}_{p,TH}$.

From our calculated $\Delta G^{\ddagger}_{p,HT}$, a $k_{p,HT}$ value of $1.1 \cdot 10^4$ L mol^{-1} s^{-1} can be derived at 298.15, which becomes $2.3 \cdot 10^4$ L mol^{-1} s^{-1} after extrapolation of $\Delta G^{\ddagger}_{p,HT}$ to the polymerization temperature. This value is actually quite close to that reported by Beueurmann *et al.* ($1.94 \cdot 10^4$ L mol^{-1} s^{-1}) in *sc*CO_2.[38] It also appears reasonable when compared for instance with those reported for tetrafluoroethylene ($7.4 \cdot 10^3$ L mol^{-1} s^{-1} at 40 °C)[41] and ethylene (470 L mol^{-1} s^{-1} at 83 °C in benzene).[42] This agreement encouraged us to continue the computational exploration using this level of theory.

c. Bond strengths.

The calculated homolytic bond dissociation enthalpy (BDE, $\Delta H°_{298.15}$), in kcal/mol, is 54.5 for CH_3CF_2-XA and 60.7 for CHF_2CH_2-XA, confirming the common perception that the bond is

stronger in the T-terminated dormant species obtained after an inverted (HH) monomer addition. The difference between the BDE of the T- and H-terminated dormant chain models almost exactly matches the energy difference of the isomeric radicals: the calculated standard enthalpy of $CHF_2CH_2^{\bullet}$ is 6.6 kcal/mol higher than that of $CH_3CF_2^{\bullet}$. Consequently, the isomeric CTA models are essentially isoenergetic (CH_3CF_2-XA is more stable than CHF_2CH_2-XA by 0.8 kcal/mol, see Figure 7).

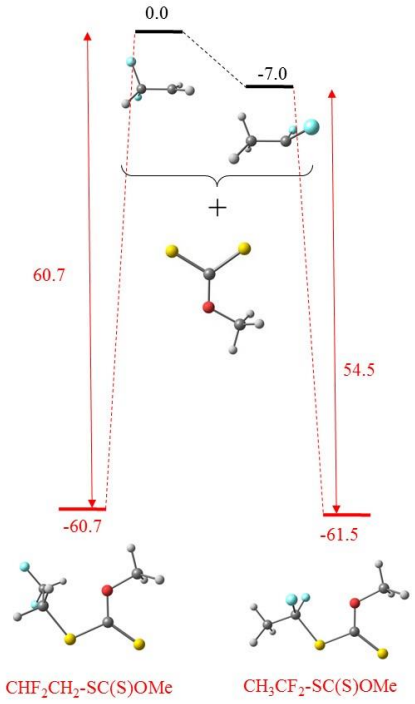

Figure 7. Relative energies and views of the optimized geometries of the isomeric $CHF_2CH_2^{\bullet}$ and $CH_3CF_2^{\bullet}$ radicals, the (MeO)C(S)S$^{\bullet}$ radical, and the corresponding adducts. The values are the standard enthalpies ($\Delta H°_{298.15}$) in kcal/mol.

d. MacroCTA $PVDF_H$-XA and $PVDF_T$-XA reactivation: degenerative and non-degenerative chain transfer.

The computational results on the chain transfer pathway are summarized in Figure 8. The $CH_3CF_2^{\bullet}$ radical, model of the more probable $PVDF_H^{\bullet}$, adds to the model of the more probable $PVDF_H$-XA macroCTA to undergo degenerative radical exchange via a symmetric CH_3CF_2-SC$^{\bullet}$(OMe)S-CF_2CH_3 intermediate, requiring only 9.0 kcal/mol in activation Gibbs energy. The symmetric intermediate is nearly isoenergetic with the fragmented starting and final degenerate CTA/radical pairs. The non-degenerative exchange leading from the same $PVDF_H$-XA model and the $CHF_2CH_2^{\bullet}$ model of $PVDF_T^{\bullet}$ to the exchanged partners CHF_2CH_2-XA and $CH_3CF_2^{\bullet}$ is thermodynamically favorable because it transforms the more energetic radical to its more stable isomer, whereas the two dormant species are approximately isoenergetic, as shown in section *c*. This exchange requires an activation Gibbs energy of 9.0 kcal/mol, *i.e.* the same as for the degenerative exchange of the $PVDF_H^{\bullet}$ radical and leads to the new partners pair, 6.1 kcal/mol lower in energy. The reverse reactivation of CHF_2CH_2-XA by $CH_3CF_2^{\bullet}$ requires a greater activation, 15.1 kcal/mol. Finally, $CHF_2CH_2^{\bullet}$ undergoes degenerative exchange with CHF_2CH_2-XA (red curve in Figure 8) with an activation barrier of 9.5 kcal/mol.

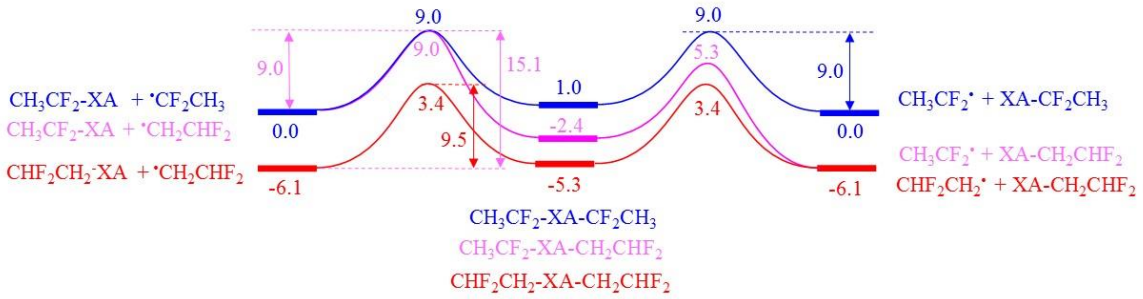

Figure 8. Energy profiles for the degenerative (H/H and T/T) and non-degenerative (H/T) radical exchange with the dormant chain. The reported values are $\Delta G^{\circ}_{298.15}$ in kcal/mol.

Discussion

The lower barrier for the $PVDF_H^{\bullet}$ degenerative chain transfer (9.0 kcal/mol) relative to HT propagation (11.9 kcal/mol, *cf.* Figures 8 and 6) agrees with the experimental observation of efficient control in degenerate transfer polymerization, so long as the growing chain remains $PVDF_H^{\bullet}$. The calculated rate constant ratio k_{CT}/k_p is $1.3 \cdot 10^2$ at 298.15 K according to the Eyring equation. After extrapolation of the two Gibbs energy barriers to the polymerization temperature (73 °C), this ratio is reduced to 70 (k_{CT} increases less than k_p at higher temperatures because the chain transfer activation barrier is characterized by a greater entropy decrease relative to the propagation activation barrier). Actually, the parameters to be compared are the rates, not the rate constants. Since $v_{CT} = k_{CT}[R^{\bullet}][CTA]$ and $v_p = k_p[R^{\bullet}][M]$, the rate ratio depends not only on the rate constant ratio but also on the concentration ratio: $v_{CT}/v_p = (k_{CT}/k_p) \cdot ([CTA]/[M])$. A problem in VDF polymerization is that the system is biphasic. The gaseous monomer is only partly dissolved in the polymerization solvent (DMC) where the CTA and macroradical react, and the monomer solubility in this condensed phase was not previously reported. Therefore, we have measured the concentration under conditions close to those of the polymerization (DMC at 70 °C and 33.1 bars, see details in the Experimental Section) and found it to be 5.2 mol/L. Thus, although this is a significant concentration, it is unlikely that all the monomer is completely dissolved in the reaction medium, hence [CTA]/[M] > 0.01 for a target DP of 100. The calculated rate ratio would predict comparable rates of chain transfer and propagation, in agreement with a reasonably controlled system.

The major point of interest in this study is the question of the $PVDF_T$-XA reactivation after an inverted monomer addition. This can in principle occur by exchange with either the more abundant $PVDF_H^{\bullet}$ radicals or with the $PVDF_T^{\bullet}$ radicals. The former has a calculated barrier of 15.1 kcal/mol for the model system. This does not mean that this reactivation cannot occur because this barrier yields a rate constant of 54 M^{-1} s^{-1} under standard conditions, by application of the Eyring relationship. However, after the endothermic non-degenerative head-tail chain transfer process ($\Delta G°_{CT,HT}$ = 6.1 kcal/mol at 298.15 K, $K_{CT,HT} = 3.4 \cdot 10^{-5}$ from the van't Hoff equation) the resulting free tail radicals can be back-trapped with a lower barrier (9.0 kcal/mol) than the subsequent addition to monomer ($\Delta G^{‡}_{p,TT}$ = 12.3 kcal/mol for the more favorable TT addition) needed to re-enter the regular $PVDF_H^{\bullet}$ chain growth process. The Gibbs energy span is thus ($\Delta G°_{CT,HT} + \Delta G^{‡}_{p,TT}$ = 18.4 kcal/mol), which can be extrapolated to 20.1 kcal/mol at 343.15 K, leading to the prediction of an effective activation rate constant $k_{Exch,TH}$ (corresponding to $Kk_{p,TT}$) for the $PVDF_T$-XA chains in VDF homopolymerization of 1.2 M^{-1} s^{-1}. Thus, in contrast to what is commonly believed, $PVDF_T$-XA chains cannot be considered dead, because the rate constant of their reactivation is significant. Using the estimated [VDF] given above (5.2 M), for instance, a pseudo-first order decay of ≈ 6 s^{-1} can be calculated for a half-life of ≈ 0.1 s, which naturally increases as the [VDF] is lowered at higher conversions. Although not negligible, this reactivation rate is nevertheless slower by 4 orders of magnitude than the reactivation of the $PVDF_H$-XA chains by the degenerative transfer and also slower than the rate at which the $PVDF_H^{\bullet}$ chains are converted to $PVDF_T^{\bullet}$ by the head-to-head propagation (Figure 6): $k_{p,HH} = 6.1 \cdot 10^{2}$ M^{-1} s^{-1}; $k_{Exch,TH}/k_{p,HH} = 2 \cdot 10^{-3}$. This is in agreement with the accumulation of the $PVDF_T$-XA macroCTA as conversion increases.

This relatively slow reactivation would also explain the loss of control observed experimentally when all xanthate-terminated PVDF chains have been converted into $PVDF_T$-XA. However, as

alluded to above, the $PVDF_T$-XA dormant chains may also be reactivated by the less numerous $PVDF_T^{\bullet}$ radicals by a degenerative tail-tail process with a lower activation barrier (9.5 kcal/mol), see Figure 8, for which the estimated rate constant at the polymerization temperature is $k_{Exch,TT}$ = $4.6 \cdot 10^5$ M^{-1} s^{-1} . The relative rates of TT degenerative exchange and TH non-degenerative exchange can be calculated as

$$v_{Exch,TT}/v_{Exch,HT} = (k_{Exch,TT}/k_{Exch,HT})\ ([PVDF_T^{\bullet}]/[PVDF_H^{\bullet}]),$$

where the $k_{Exch,TT}/k_{Exch,HT}$ rate constant ratio is $3.8 \cdot 10^5$ and $[PVDF_T^{\bullet}]/[PVDF_H^{\bullet}]$ can be estimated as 0.04, considering a proportion of HH addition of 4 % at 343 K. Thus, this calculation yields $v_{Exch,TT}/v_{Exch,HT} = 1.5 \cdot 10^4$. Counterintuitively, and in spite of the non-negligible rate constant of the non-degenerate reactivation of $PVDF_T$-XA by $PVDF_H^{\bullet}$ radicals, the computational investigation suggests that the $PVDF_T$-XA chains are actually reactivated much faster by the minority $PVDF_T^{\bullet}$ radicals.

The controlled nature of the VDF polymerization can be appreciated from the comparison of the rate of propagation and the rate of exchange. The rate of propagation would still be dominated by the HT addition, after liberation of the dormant $PVDF_T$ chain which is converted to a $PVDF_H^{\bullet}$ radical by the first TT addition: $v_{p,HT}$ = $(1.9 \cdot 10^4$ M^{-1} $s^{-1})[PVDF_H^{\bullet}][VDF]$. The faster rate of exchange is $v_{Exch,TT}$ = $(4.6 \cdot 10^5$ M^{-1} $s^{-1})[PVDF_T^{\bullet}][PVDF_T\text{-XA}]$. By introducing $[PVDF_T^{\bullet}]$ = $0.04[PVDF_H^{\bullet}]$, we derive $v_{p,HT}/v_{Exch,TT} \sim 1.0 \cdot [VDF]/[PVDF_T\text{-XA}]$. Given that the monomer concentration is greater than the $PVDF_T$-XA concentration, even when the monomer is partially consumed and 100% of the macroCTA is in the $PVDF_T$-XA form, this calculation predicts a much faster propagation than the rate of radical exchange, thus loss of control.

Scheme 2 summarizes all the findings of this study. The VDF RAFT polymerization in DMC gradually leads to the accumulation of $PVDF_T$-XA macroCTA (equations (4) and (7), Scheme 2) and undergoes a mechanistic transition from a controlled DT mechanism to an uncontrolled DT mechanism (a DT mechanism too slow to provide control) when no more $PVDF_H$-XA macroCTA remains. During the uncontrolled phase of the polymerization, DT still occurs, but only between the $PVDF_T$-XA macroCTA and the $PVDF_T^{\bullet}$ radicals, which are present at low concentration (equation (8), Scheme 2). The non-DT exchange (equation (7), Scheme 2), although theoretically non negligible, likely does not occur due to a much lower rate compared to the DT exchange between HH-terminated PVDF chains. In addition, during that phase, transfer to DMC (equations (9) and (10), Scheme 2) becomes more prominent and reactions such as chain initiation by DMC radical (equation (13), Scheme 2) or irreversible exchange between DMC radical and PVDF-XA (equations (11) and (12), Scheme 2), which were almost insignificant during the controlled phase of the polymerization, occur more frequently with a growing impact on the PVDF functionality.

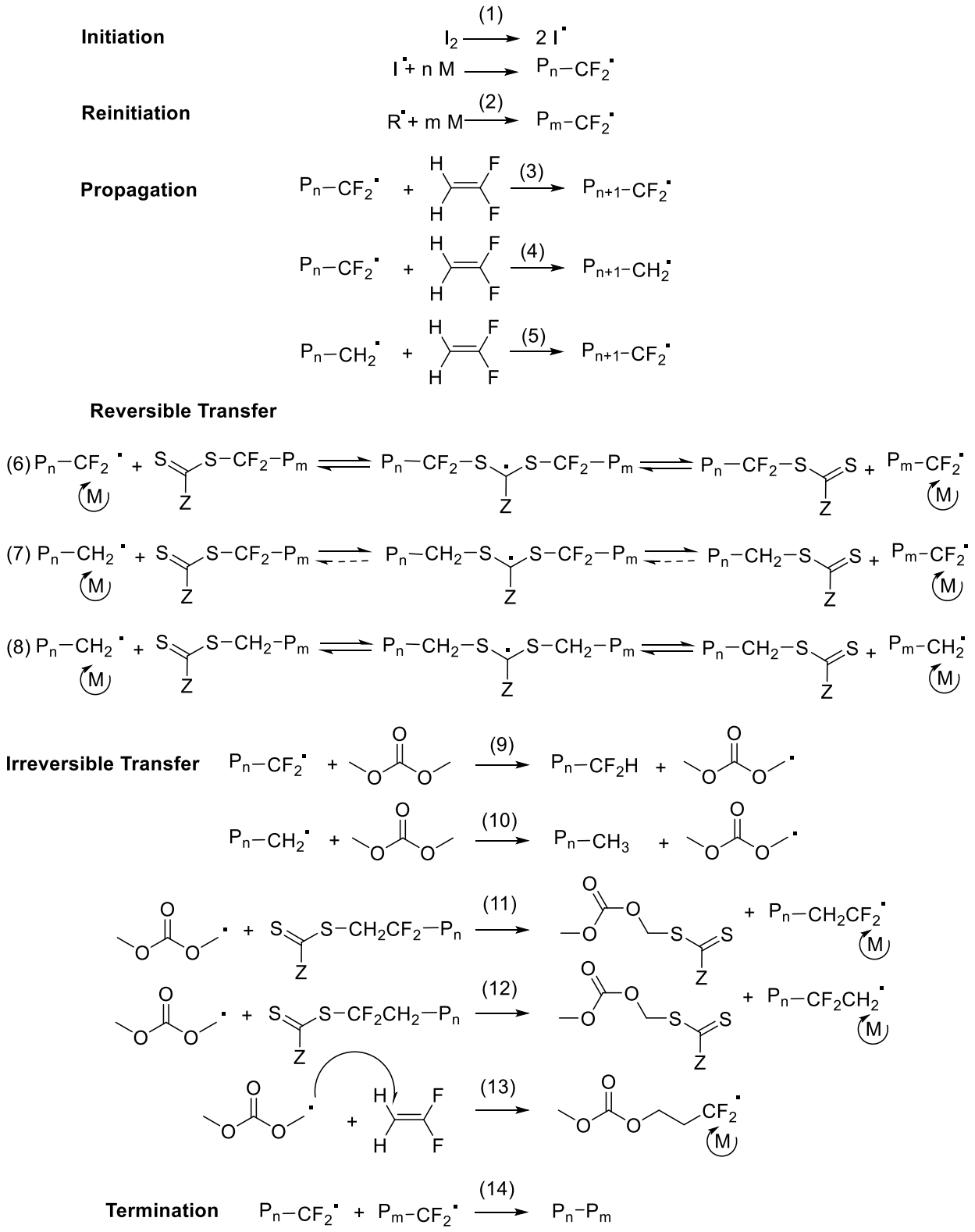

Scheme 2. Reactions occurring during the RAFT polymerization of VDF.

CONCLUSION

This study demonstrates that RAFT polymerization of VDF can be used to efficiently prepare well-defined PVDF with high end-group functionality and over a relatively large range of molar masses in spite of the unavoidable accumulation of less reactive $PVDF_T$-XA chains formed by head-to-head VDF addition. However, well-defined high-molar-mass PVDF can only be prepared at relatively low conversions (< ca. 30 %). Indeed, this work shows that controlled polymerization, via a DT mechanism with a sufficiently fast radical exchange, only occurs while regioregularly ended $PVDF_H$-XA chains are still present. When all the xanthate-terminated PVDF chains have been converted into $PVDF_T$-XA chains, the degenerative transfer mechanism slows down dramatically, although it does not stop completely, resulting in a significant loss of polymerization controllability, as the xanthate group exchange rate becomes slower than the propagation rate. DFT calculations suggest that, contrarily to common belief, the $PVDF_T$-XA dormant chains are not dead and can be reactivated at a non-negligible rate. They further indicate that this reactivation occurs primarily via degenerative transfer with the $PVDF_T^{\bullet}$ radicals, in spite of their lower concentrations. In addition, the present study suggests that chain transfer to the solvent, DMC, may be responsible for additional detrimental reactions after the full conversion of all the PVDF active chains into the less reactive $PVDF_T$-XA chains. The resulting DMC radicals seem to both readily initiate new PVDF chains and exchange with the $PVDF_T$-XA chains, thus decreasing the overall end-group functionality of the final PVDF. In summary, the RAFT polymerization of VDF proceeds through two consecutive regimes marked by a sharp kinetic transition. In the first regime both $PVDF_H$-XA and $PVDF_T$-XA coexist and polymerize at different rates. $PVDF_H$-XA chains are involved in fast DT mechanism which leads to PVDF with low dispersity, while the $PVDF_T$-XA chains polymerize

via a much slower DT mechanism which causes a broadening of the molar masses distribution of the resulting PVDF. In the second part of the polymerization, only the $PVDF_T$-XA chains remain, the slower exchange of which is not sufficient to ensure good control of the polymerization. This study provides a much better understanding of the RAFT polymerization of VDF and clearly delineates the limits of this polymerization technique. Finally, it unambiguously refutes the common belief that the $PVDF_T$-XA chains cannot be reactivated, and thus questions the robustness of other RDRP techniques such as ITP, which are also affected by chain inversions of monomers such as vinyl acetate and VDF.

ASSOCIATED CONTENT

Supporting Information: Equations used for calculation of end-group proportions and functionality, Plots of $Ln([CTA]_0/[CTA])$ versus $Ln ([VDF]_0/[VDF]$, ^1H and ^{19}F NMR spectra of representative polymers, Energies, enthalpies, Gibbs energies, Cartesian coordinates and views of all optimized geometries. This material is available free of charge via the Internet at http://pubs.acs.org.

AUTHOR INFORMATION

Corresponding Authors

*E-mail: vincent.ladmiral@enscm.fr; rinaldo.poli@lcc-toulouse.fr.

Notes

The authors declare no competing financial interest.

ACKNOWLEDGMENT

The authors thank Arkema (Pierre Bénite, France) for providing VDF, and the French Ministry of Science and Technology for the Ph.D. grant attributed to MG.

REFERENCES

1. (a) Smith, D. W.; Iacono, S. T.; Suresh, S. I. In *Handbook of Fluoropolymers Science and Technology;* John Wiley & Sons, Inc: New York**, 2004.** (b) Gardiner, Fluoropolymers: Origin, Production, and Industrial and Commercial Applications *J. Aust. J. Chem.* **2015**, *68*, 13-22.

2. Ameduri, B.; Boutevin, B. *Well-Architectured Fluoropolymers: Synthesis, Properties and Applications*; Elsevier: Amsterdam**, 2004.**

3. Tatemoto, M. *In The First Regular Meeting of Soviet-Japanese Fluorine Chemists,* Tokyo, Japan, February 15−16, **1979.**

4. Dolbier, W. R. Jr. Structure, Reactivity and Chemistry of Fluoroalkyl Radicals *Chem. Rev.* **1996**, *96*, 1557-1584.

5. Cui, Z.; Drioli, E.; Lee, Y. M. Recent progress in fluoropolymers for membranes *Prog. Polym. Sc.* **2014**, *39*, 164-198.

6. Soulestin, T.; Ladmiral, V.; Lannuzel, T.; Domingues Dos Santos, F.; Ameduri, B. Importance of Microstructure Control for Designing New Electroactive Terpolymers Based on Vinyllidene Fluoride and Trifluoroethylene *Macromolecules* **2015**, *48*, 7861-7871.

7. Katsouras, I.; Asadi, K.; Li, M.; van Driel, T. B.; Kjær, K. S.; Zhao, D.; Lenz, T.; Gu, Y.; Blom, P. W. M.; Damjanovic, D.; Nielsen, M. M.; de Leeuw, D. M. The negative piezoelectric effect of the ferroelectric polymer poly(vinylidene fluoride) *Nat. Mater*. **2016**, *15*, 78-84.

8. Ameduri, B, From Vinylidene Fluoride (VDF) to the Applications of VDF-Containing Polymers and Copolymers: Recent Developments and Future Trends *Chem. Rev.* **2009**, *109*, 6632-6686.

9. Ameduri, B. Controlled radical (Co)polymerization of Fluoromonomers *Macromolecules* **2010**, *43*, 10163-10184.

10. David ; G.; Boyer, C .; Tonnar, J .; Ameduri, B .; Lacroix-Desmazes, P .; Boutevin, B. Use of Iodocompounds in Radical Polymerization *Chem. Rev.* **2006**, *106*, 3936-3962.

11. Hill, M. R. Carmean, R. N.; Sumerlin, B. S. Expanding the Scope of RAFT Polymerization: recent Advances and New Horizons *Macromolecules* **2015**, *48*, 5459-5469.

12. Liu, L.; Lu, D.; Wang, H.; Dong, Q.; Wang, P.; Bai, R. Living/controlled free radical copolymerization of chlorotrifluoroethene and butyl vinyl ether under ^{60}Co γ-ray irradiation in the presence of S-benzyl O-ethyl dithiocarbonate *Chem. Commun*. **2011**, *47*, 7839-7841.

13. Kostov, G.; Boschet, F.; Buller, J.; Badache, L.; Brandsadter, S.; Ameduri, B. First Amphiphilic Poly(vinylidene fluoride –co-3,3,3-trifluoropropene)-b-oligo(vinyl

alcohol) Block Copolymers as potential Nonpersistent Fluorosurfactants from Radical Polymerization Controlled by Xanthate *Macromolecules* **2011**, *44*, 1841−1855.

14. Asandei, A. D.; Adebolu, O. I.; Simpson, C. P. Mild Temperature $Mn_2(CO)_{10}$-Photomediated Controlled Radical Polymerization of Vinylidene Fluoride and Synthesis of Well-defined Poly(vinylidene fluoride)block Copolymers*J. Am. Chem. Soc*. **2012**, *134*, 6080−6083.

15. Girard, E.; Marty, J. D.; Ameduri, B.; Destarac, Direct synthesis of Vinylidene Fluoride-Based Amphiphilic Diblock Copolymers by RAFT/MADIX Polymerization M. *ACS Macro Lett.* **2012**, *1*, 270−274.

16. Wang, P.; Dai, J.; Liu, L.; Dong, Q.; Jinand B.; Bai R. Xanthate-mediated living/controlled radical copolymerization of hexafluoropropylene and butyl vinyl ether under ^{60}Co γ-ray irradiationand preparation of fluorinated polymrs end-capped with fluoroalkyl sulfonic acid group *Polym. Chem*. **2013**, *4*, 1760-1764.

17. Asandei, A. D.; Adebolu, O. I.; Simpson, C. P.; Kim, Visible-Light Hypervalent Iodide Carboxylate Photo(trifluoro)methylations and Controlled Radical Polymerization of Fluorinated Alkenes J. S. *Angew. Chem., Int. Ed*. **2013**, *52*, 10027−10030.

18. Patil, Y.; Ameduri, B. First RAFT/MADIX copolymerization of *tert*-butyl 2-trifluoromethacrylate with vinylidene fluoride controlled by xanthate *Polym. Chem*. **2013**, *4*, 2783−2799.

19. Guerre, M.; Campagne, B.; Gimello, O.; Parra, K.; Ameduri, B.; Ladmiral, V. Deeper Insight into the MADIX polymerization of Vinylidene Fluoride *Macromolecules* **2015**, *48*, 7810-7822.

20. Asandei, A. D. Photomediated Controlled Radical Polymerization and Block Copolymerization of Vinylidene Fluoride *Chem. Rev.* **2016**, *116*, 2244-2274.

21. Guerre, M.; Ameduri, B.; Ladmiral, V. One-pot synthesis of poly(vinylidene fluoride) methacrylate macromonomers *via* thia-Michael *Polym. Chem* **2016**, *7*, 441-450.

22. Boyer, C.; Valade, D.; Sauguet, L.; Ameduri, B.; Boutevin, B. Iodine Transfer Polymerization (ITP) of Vinylidene Fluoride (VDF). Influence of the Defect of VDF Chaining on the Control of ITP *Macromolecules* **2005**, *38*, 10353-10362.

23. X. Liu, O. Coutelier, S. Harisson, T. Tassaing, J-D. Marty, M. Destarac, Enhanced Solubility of Polyvinyl Esters in $scCO_2$ by Means of Vinyl Trifluorobutyrate Monomer *ACS Macro Lett.* **2015**, *4*, 89-93.

24. Frisch, M. J.; Trucks, G. W.; Schlegel, H. B.; Scuseria, G. E.; Robb, M. A.; Cheeseman, J. R.; Scalmani, G.; Barone, V.; Mennucci, B.; Petersson, G. A.; Nakatsuji, H.; Caricato, M.; Li, X.; Hratchian, H. P.; Izmaylov, A. F.; Bloino, J.; Zheng, G.; Sonnenberg, J. L.; Hada, M.; Ehara, M.; Toyota, K.; Fukuda, R.; Hasegawa, J.; Ishida, M.; Nakajima, T.; Honda, Y.; Kitao, O.; Nakai, H.; Vreven, T.; Montgomery, J., J. A.; Peralta, J. E.; Ogliaro, F.; Bearpark, M.; Heyd, J. J.; Brothers, E.; Kudin, K. N.; Staroverov, V. N.; Kobayashi, R.; Normand, J.; Raghavachari, K.; Rendell, A.; Burant, J. C.; Iyengar, S. S.; Tomasi, J.; Cossi, M.; Rega, N.; Millam, N. J.; Klene, M.; Knox, J. E.; Cross, J. B.; Bakken, V.; Adamo, C.; Jaramillo, J.; Gomperts, R.; Stratmann, R. E.; Yazyev, O.;

Austin, A. J.; Cammi, R.; Pomelli, C.; Ochterski, J. W.; Martin, R. L.; Morokuma, K.; Zakrzewski, V. G.; Voth, G. A.; Salvador, P.; Dannenberg, J. J.; Dapprich, S.; Daniels, A. D.; Farkas, Ö.; Foresman, J. B.; Ortiz, J. V.; Cioslowski, J.; Fox, D. J. Gaussian 09, Revision D.01; Gaussian, Inc.: Wallingford CT, 2009.

25. Bryantsev, V. S.; Diallo, M. S.; Goddard, W. A., Calculation of Solvation Free Energies of Charged Solutes Using Mixed Cluster/Continuum Models III *J. Phys. Chem. B* **2008**, *112*, 9709-9719.

26. O'Brien, J. L.; Gornick, F. Chain Transfer in the Polymerization of Methyl Methacrylate. I. Transfer with Monomer and Thiols. The Mechanism oft he Termination reaction at 60°C *J. Am. Chem. Soc.* **1955**, *77*, 4757.

27. (a) G. Moad, E. Rizzardo, S. H. Thang, Living Radical Polymerization by the RAFT Process- A Second Update *Aust. J. Chem*. **2009**, *62*, 1402. (b) E. Bicciocchi, Y. K. Chong, L. Giorgini, G. Moad, E. Rizzardo, S. H. Thang, Substituents Effects on RAFT Polymerization with Benzyl Aryl Trithiocarbonates *Macromol. Chem. Phys.* **2010**, 211, 529. (c) D. J. Keddie, C. Guerrero-Sanchez, G. Moad, R. J. Mulder, E. Rizzardo, S. H. Thang, Chain Transfer Kinetics of Acid/Base Switchable *N*-Aryl-*N*-Pyridyl Dithiocarbamate RAFT Agents in Methyl Acrylate, N-Vinylcarbazole and Vinyl Acetate Polymerization *Macromolecules* **2012**, *45*, 4205.

28. Boyer, C.; Valade, D.; Ameduri, B.; Lacroix Desmazes, P.; Boutevin, B. Kinetics od the iodine transfer polymerization of vinylidene fluoride *J. Polym. Sci., Part A: Polym. Chem.* **2006**, *44*, 5763-5777.

29. Guerre, M.; Lopez, G.; Soulestin, T.; Totée, C.; Ameduri, B.; Silly, G.; Ladmiral, V. A Journey into the Microstructure of PVDF Made by RAFT *Macromol. Chem. Phys.* **2016** DOI: 10.1002/macp.201600109.

30. G. Pound, J. B. McLeary, J. M. McKenzie, R. F. M. Lange, B. Klumperman, In-Situ NMR Spectroscopy for Probing the Efficiency of RAFT/MADIX Agents *Macromolecules* **2006**, *39*, 7796

31. Stenzel, M. H.; Cummins, L.; Roberts, G.E.; Davis, T. P.; Vana, P.; Barner-Kowollik, C. Xanthate Mediated Living Polymerization of Vinyl Acetate: A Systematic Variation in MADIX/RAFT Agent Structure *Macromol. Chem. Phys.* **2003**, *204*, 1160-1168.

32. Pladis, P.; Alexopoulos, A. H.; Kiparissides, K. Mathematical Modeling and Simulation of Vinylidene Fluoride Emulsion Polymerization *Ind. Eng Chem Res* **2014**, *53*, 7352-7364.

33. (a) Guiot, J.; Ameduri, B.; Boutevin, B. Radical Homopolymerization of Vinylidene Fuoride Initiated by *tert*-Butyl Peroxypivalate. Investigation of the Microstruture by ^{19}F and ^{1}H NMR Spectroscopies and Mechanisms. *Macromolecules* **2002**, *35*, 8694−8707.

(b) Mladenov, G.; Ameduri, B.; Kostov, G.; Mateva, R. Synthesis and characterization of fluorinated telomers containing vinylidene hexafluoropropene from 1,6-diiodoperfluorohexane *J. Polym. Sci., Part A: Polym. Chem.* **2006**, 44, 1470-1485.

34. (a) Coote, M. L.; Radom, L. Ab initio Evidence for Slow Fragmentation, in RAFT Polymerization *J. Am. Chem. Soc*. **2003**, *125*, 1490-1491. (b) Coote, M. L. Ab Initio Study of the Addition-Fragmentation Equilibrium in RAFT Polymerization: When is

Polymerization Retarded? *Macromolecules* **2004**, *37*, 5023-5031. (c) Coote, M. L.; Radom, L. Substituent Effects in Xanthate-Mediated Polymerization of Vinyl Acetate: Ab Initio Evidence for an Alternative Fragmentation Patway *Macromolecules* **2004**, *37*, 590-596. (d) Coote, M. L. The kinetics of Addition and Fragmentation in reversible Addition Fragmentation Chain Transfer Polymerization: An Ab initio Study *J. Phys. Chem. A* **2005**, *109*, 1230-1239. (e) Coote, M. L.; Henry, D. J. Effect of Substituents on Radical Stability in Reversible Addition Fragmentation Chain Transfer Polymerization: An ab Initio Study *Macromolecules* **2005**, *38*, 1415-1433. (f) Coote, M. L.; Henry, D. J. Computer-Aided Design of a Destabilized RAFT Adduct Radical: Toward Improved RAFT Agents Styrene-*block*-Vinyl Acetate Copolymers *Macromolecules* **2005**, *38*, 5774-5779. (g) Matyjaszewski, K.; Poli, R. Comparison of Bond Dissociation Energies of Dormant Species Relevant to Degenerative Transfer and Atom Transfer Radical Polymerization *Macromolecules* **2005**, *38*, 8093-8100. (h) Coote, M. L.; Krenske, E. H.; Izgorodina, E. I. Compitational Studies of RAFT Polymerization-Mechanistic Insights and Practical Applications *Macromol. Rapid Comm.* **2006**, *27*, 473.(i) Abreu, C. M. R.; Mendonça, P. V.; Serra, A. C.; Coelho, J. F. J.; Anatoliy, V. P.; Gryn'ova, G.; Coote, M. L.; Guliashvili, T. Reversible Addition-Fragmentation Chain Transfer Polymerization of Vinyl Chloride *Macromolecules* **2012**, *45*, 2200-2208.

35. (a) Gillies, M. B.; Matyjaszewski, K.; Norrby, P.-O.; Pintauer, T.; Poli, R.; Richard, P. A DFT Study of R-X Bond Dissociation Enthalpies of Relevance to the Initiation process of Atom Radical Polymerization *Macromolecules* **2003**, *36*, 8551-8559. (b) Lin, C. Y.; Coote, M. L.; Petit, A.; Richard, P.; Poli, R.; Matyjaszewski, K. Ab Initio Study of the Penultimate effect for the ATRP Activation Step Using Propylene, Methyl

Acrylate, and Methyl Methacrylate Monomers *Macromolecules* **2007**, *40*, 5985-5994. (c) Braunecker, W. A.; Brown, W. C.; Morelli, B.; Tang, W.; Poli, R.; Matyjaszewski, K. Origin of Activity in Cu-, Ru-, and Os-Mediated Radical Polymerization *Macromolecules* **2007**, *40*, 8576-8585. (d) Tang, W.; Kwak, Y.; Braunecker, W.; Tsarevsky, N. V.; Coote, M. L.; Matyjaszewski, K. Understanding Atom Transfer Radical Polymerization : Effect od Ligand and Initiator Structures on the Equilibrium Constants *J. Am. Chem. Soc.* **2008**, *130*, 10702-10713. (e) Zhang, Y.; Schröder, K.; Kwak, Y.; Krys, P.; Morin, A. N.; Pintauer, T.; Poli, R.; Matyjaszewski, K. Reversible-Deactivation Radical Polymerization of Methyl Methacrylate and Styrene Mediated by Alkyl Dithiocarbamates and Copper Acetylacetonates *Macromolecules* **2013**, *46*, 5512-5519.

36. a) Maria, S.; Kaneyoshi, H.; Matyjaszewski, K.; Poli, R. Effect of Electron Donors on the Radical Polymerization of Vinyl Acetate Mediated by [$Co(acac)_2$] : Degenerative Transfer versus Reversible Homolytic Cleavage of an Organocobalt(III) Complex *Chem. Eur. J.* **2007**, *13*, 2480. (b) Debuigne, A.; Champouret, Y.; Jérôme, R.; Poli, R.; Detrembleur, Mechanistic Insights into the Cobalt-Mediated Radical Polymerization (CMRP) of Vinyl Acetate with Cobalt(III) adducts as Initiators C. *Chem. Eur. J.* **2008**, *14*, 4046-4059. (c) Debuigne, A.; Michaux, C.; Jérôme, C.; Jérôme, R.; Poli, R.; Detrembleur, C. Cobalt-Mediated Radical Polymerization of Acrylonitrile Kinetics Investigations and DFT Calculations *Chem. Eur. J.* **2008**, *14*, 7623-7637. (d) Champouret, Y.; Baisch, U.; Poli, R.; Tang, L.; Conway, J. L.; Smith, K. M. Homolytic Bond Strengths and Formation Rates in Half-Sandwich Chromium Alkyl Complexes: Revelance for Controlled Radical Polymerization *Angew. Chem. Int. Ed. Engl.* **2008**,

47, 6069-6072. (e) Debuigne, A.; Poli, R.; De Winter, J.; Laurent, P.; Gerbaux, P.; Dubois, P.; Wathelet, J.-P.; Jérôme, C.; Detrembleur, C. Cobalt-Mediated Radical Coupling (CMRC): An Unusual Route to Midchain-Functionalized Symmetrical Macromolecules *Chem. Eur. J.* **2010**, *16*, 1799-1811. (f) Debuigne, A.; Poli, R.; De Winter, J.; Laurent, P.; Gerbaux, P.; Wathelet, J.-P.; Jérôme, C.; Detrembleur, C. Effective Cobalt-Mediated Radical Coupling (CMRC) of Poly(vinyl acetate) and Poly(*N*-vinylpyrrolidone) (Co)polymer Precusors *Macromolecules* **2010**, *43*, 2801-2813. (g) Champouret, Y.; MacLeod, K. C.; Baisch, U.; Patrick, B. O.; Smith, K. M.; Poli, R. Cyclopentadienyl Chromium β-Diketiminate Complexes: Initiators, Liguand Steric Effects, and Deactivation Processes in the Controlled Radical Polymerization of Vinyl Acetate *Organometallics* **2010**, *29*, 167-176. (h) Champouret, Y.; MacLeod, K. C.; Smith, K. M.; Poli, R. Controlled Radical Polymerization of Vinyl Acetate with Cyclopentadienyl Chromium β-Diketiminate Complexes: ATRP or OMRP *Organometallics* **2010**, *29*, 3125-3132. (i) Debuigne, A.; Morin, A. N.; Kermagoret, A.; Piette, Y.; Detrembleur, C.; Jérôme, C.; Poli, R. Key Role of Intramolecular Metal Chelation and Hydrogen Bonding in the Cobalt-Mediated Radical Polymerization of *N*-Vinyl Amides *Chem. Eur. J.* **2012**, *18*, 12834-12844. (j) Piette, Y.; Debuigne, A.; Jérôme, C.; Bodart, V.; Poli, R.; Detrembleur, C. Cobalt-mediated radical (co)polymerization of vinyl chloride and vinyl acetate *Polym. Chem.* **2012**, *3*, 2880-2891. (k) Morin, A. N.; Detrembleur, C.; Jérôme, C.; Tullio, P. D.; Poli, R.; Debuigne, A. Effect of Head-to-Head Addition in Vinyl Acetate Controlled Radical Polymerization : Why Is $Co(acac)_2$-Mediated Polymerization so Much Better ? *Macromolecules* **2013**, *46,* 4303-4312.

37. Abreu, C. M. R.; Mendonça, P.V.; Serra, A. C.; Noble, B. B.; Guliashvili, T.; Nicolas, J.; Coote, M. L.; Coelho, J. F. J. Nitroxide-Mediated Polymerization of Vinyl Chloride at low Temperature : Kinetic and Computational Studies *Macromolecules* **2016**, *49*, 490-498.

38. Siegmann, R.; Drache, M.; Beuermann, S. PropagationRate Coefficient for Vinylidene Fluoride Homopolymerizations *Macromolecules,* **2013**, *46*, 9507-9514.

39. (a) Bachmann, M. A.; Gordon, W. L.; Koening, J. L.; Lando, J. B. An infrared study of phase-III Poly(vinylidene Fluoride) *J. Appl. Phys.* **1979**, *50*, 6106. (b) Mattern, D. E.; Fu-Tyan, L.; Hercules, D. M. Laser mass spectrometry of poly(fluoroethylenes) *Anal. Chem* **1984**, *56*, 2762-2769. (c) Lovinger, A. J.; Davis, D. D.; Cais, R.E.; Kometani, J. M. The role of molecular defects on the structure and phase transition of poly(vinylidene fluoride) *Polymer* **1987**, *28*, 617-626.

40. Laflamme, P.; Porzio, F.; Ameduri, B.; Soldera, A. Characterization of the telomerization reaction path for vinylidene fluoride with CCl3 radicals *Polym. Chem.* **2012**, *3*, 652-657.

41. A. N. Plyusnin, N. M. Chirkor, *Theor. Eksp. Khimiya*, **1966**, *2*, 777.

42. Z. Litia, Z. Machacek, The kinetic of radical polymerization of ethylene. II. Determination of the Kinetic coefficients *J. Polym. Sci.* **1959**, *38*, 459.

Insert Table of Contents Graphic and Synopsis Here